Bioconjugate Chemistry

Article

Cite This: Bioconjugate Chem. XXXX, XXX, XXX−XXX

pubs.acs.org/bc

SERS-Based Quantification of Biomarker Expression at the Single Cell Level Enabled by Gold Nanostars and Truncated Aptamers

Manjari Bhamidipati,[†] Hyeon-Yeol Cho,[∥] Ki-Bum Lee,[∥,‡] and Laura Fabris*[,§]

[†]Department of Biomedical Engineering, Rutgers University, 599 Taylor Road, Piscataway, New Jersey 08854, United States

[∥]Department of Chemistry and Chemical Biology, Rutgers University, 610 Taylor Road, Piscataway, New Jersey 08854, United States

[‡]College of Pharmacy, Kyung Hee University, 26 Kyunghee-daero, Seoul 02447, Republic of Korea

[§]Department of Materials Science and Engineering, Rutgers University, 607 Taylor Road, Piscataway, New Jersey 08854, United States

Supporting Information

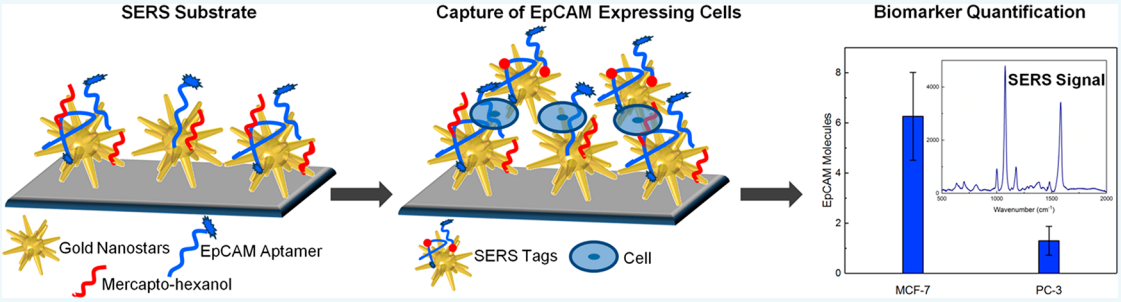

ABSTRACT: Surface-enhanced Raman spectroscopy (SERS)-based biosensors have been used increasingly over the past few years for cancer detection and diagnosis. SERS-based imaging offers excellent sensitivity and has advantages over other detection techniques such as fluorescence. In this study, we developed a novel biosensor to detect the cancer biomarker epithelial cell adhesion molecule (EpCAM) and quantify its expression at the single cell level. EpCAM is one of the most commonly expressed markers on a variety of cancer cells; importantly it has been suggested that reduction of its expression levels could be associated with the epithelial to mesenchymal transition (EMT) and thus to the onset of metastasis. Therefore, monitoring variations in expression levels of this membrane biomarker would improve our ability to monitor cancer progression. The described substrate-based biosensor was developed employing gold nanostars functionalized with EpCAM aptamer molecules and was able to quantify subnanomolar concentrations of EpCAM protein in solution. Importantly, we demonstrated its use to quantify EpCAM expression on the surface of two cancer cells, MCF-7 and PC-3. We also compared the binding efficiency of two EpCAM DNA aptamers of different lengths and observed a substantial improvement in the sensitivity of detection by employing the shorter aptamer sequence, probably due to the reduced number of conformations possible at room temperature with the truncated oligonucleotide. Detailed characterization of the substrates was carried out using both SERS maps and atomic force microscopy. These substrate-based diagnostic devices promise to be relevant for monitoring phenotype evolutions in cancer cells, blood, and other bodily fluids, thus improving our ability to follow in real time disease onset and progression.

INTRODUCTION

Nanotechnology-based approaches have shown great promise for diagnosis and prognosis of cancer and have led to a reduction in cancer-related mortality owing in particular to their ability to improve the design of disease-specific treatments.[1] A variety of cancer biomarkers such as proteins, nucleic acids, and small metabolites, as well as tumor cells offer valuable insight into cancer progression, as their expression allows for monitoring a response to therapy much earlier than more established techniques such as MRI or CT, in that they do not require changes in the tumor mass to become measurable to determine treatment efficacy.[2] Among these biomarkers, the membrane-expressed epithelial cell adhesion molecule (EpCAM) is one of the most abundantly used markers for detecting a broad variety of cancers such as colon, gastric, prostate, ovarian, lung, and breast.[3,4] Down-regulation of EpCAM, in addition to overexpression of mesenchymal markers, has been associated with the onset of metastasis.[5] However, the detection of variations in EpCAM expression with high sensitivity and selectivity remains challenging.

SERS is an ultrasensitive vibrational spectroscopic technique that has been used for biosensing and diagnostics.[6] SERS-

Received: June 7, 2018
Revised: August 9, 2018
Published: August 15, 2018

DOI: 10.1021/acs.bioconjchem.8b00397
Bioconjugate Chem. XXXX, XXX, XXX−XXX

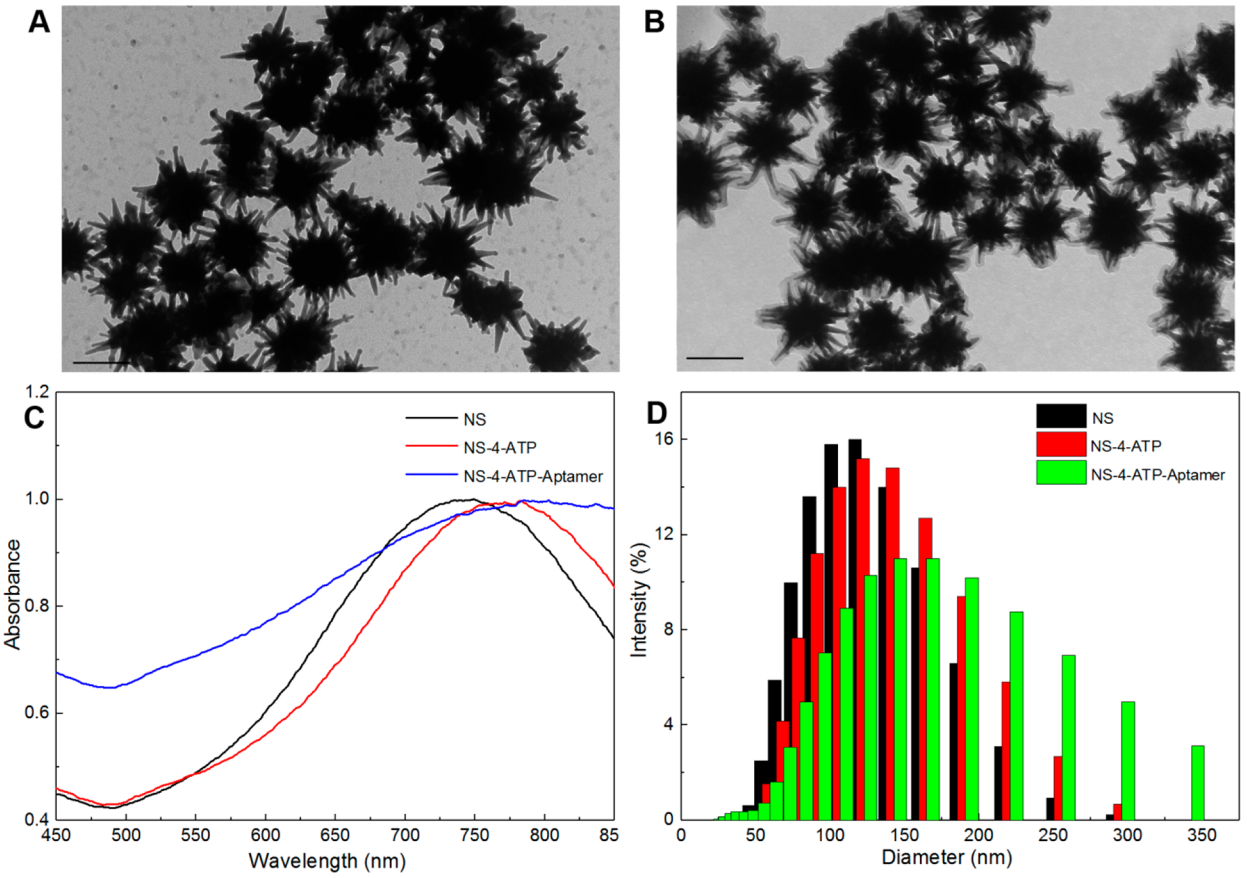

Figure 1. Assessment of nanostar properties and functionalization was carried out with multiple techniques. (A) and (B) show transmission electron (TEM) micrographs of (A) as synthesized gold nanostars and (B) nanostars functionalized with 4-aminothiophenol and EpCAM aptamer. Scale bars are 100 nm. (C) shows the UV−visible spectra of as-synthesized gold nanostars, 4-ATP-coated nanostars, and 4-ATP- and EpCAM aptamer-coated nanostars. (D) shows the relative dynamic light scattering (DLS) data, which provide size distributions in Milli-Q water at room temperature of as-synthesized nanostars, nanostars functionalized with 4-ATP, and with 4-ATP and EpCAM aptamer.

based imaging offers the advantages of narrow Raman peak width with no spectral overlap, minimal photobleaching, and effective multiplexing, and has been shown to outperform fluorescence.[7] SERS-based approaches employing tags have recently demonstrated to be powerful tools for effective identification of tumor margins *in vivo* and improved tumor excision in murine models of glioblastoma and breast cancer.[8,9] SERS tags are composed of a plasmonic nanoparticle (NP) like gold, Raman reporter molecules, and targeting moieties such as antibodies, peptides, and aptamers. The presence of the reporter near the plasmonic nanoparticle greatly enhances its Raman signal. The shape of the NP influences its optical properties and hence the brightness of the tag; in particular, nanoparticles presenting edges and corners have been shown to lead to the highest near-field enhancements and thus to the highest sensitivities.[7] Gold nanostars, particularly, have shown excellent enhancement factors with ultrasensitivity that can enable single molecule detection.[10] The highly specific recognition enabled by SERS tags is provided via the use of aptamers or antibodies. Aptamers are a new class of targeting moieties and are single-stranded DNA or RNA molecules isolated through SELEX (Systematic Evolution of Ligands by Exponential enrichment).[11,12] Their ease of synthesis and manipulation with different functional groups[13] enables targeting a wide range of biomarkers with high affinity owing to their ability to fold into secondary and tertiary structures. They offer advantages of low immunogenicity, long-term stability both in solution and as a dry powder, and rapid tissue penetration.[14−17]

In this study, we developed a SERS-based biosensor, comprising gold nanostars and EpCAM aptamers that enabled us to detect small changes in the concentration of soluble EpCAM protein and in the expression of EpCAM in individual cancer cells with high sensitivity and selectivity. For this purpose, we initially used a 48 base pair (bp) EpCAM DNA aptamer, SYL3C, that was developed by Song et al.[18] for a variety of cancer cells expressing EpCAM on their surface. The biosensor was developed by functionalizing substrates with gold nanostars and EpCAM aptamer molecules. Varying concentrations of EpCAM protein were added, and their SERS response was measured by adding SERS tags comprising the Raman reporter (4-aminothiophenol, 4-ATP) and the EpCAM aptamer in a sandwich fashion. Detailed characterization of the substrates was carried out using SERS maps, atomic force microscopy (AFM), and scanning electron microscopy (SEM). SERS tags were characterized using dynamic light scattering (DLS), zeta potential, and transmission electron microscopy (TEM). In order to improve the sensitivity of the assay, the substrates were also tested with a shorter 17-bp EpCAM aptamer, EpA, developed by Macdonald et al., which was suggested to provide improved target recognition and binding.[19] The substrates with the shorter aptamer were characterized in a similar manner. Most of the aptamers against cancer biomarkers are developed in cells and

DOI: 10.1021/acs.bioconjchem.8b00397
Bioconjugate Chem. XXXX, XXX, XXX−XXX

are used to detect membrane-embedded biomarkers. Furthermore, due to the substantially more limited application of aptamers in bioassays or cell studies, a significantly lower pool of aptamers is available on the market for the development of suitable assays for early disease detection. Thus, we were interested in determining whether these aptamers could be used to detect both soluble and membrane-embedded proteins. Membrane-embedded protein markers, because of their position across the phospholipid bilayer, necessarily possess an epitope presentation that is different from that of their soluble counterparts, thus the use of aptamers developed via cell-SELEX to detect soluble proteins might not necessarily lead to the sensitive detection of soluble EpCAM (and vice versa). For these reasons, we wanted to first assess the effectiveness of this cell-based EpCAM aptamer for the detection of low concentrations of soluble EpCAM proteins in solution. Upon verification that changes in epitope presentation due to steric hindrance and/or interactions with the surrounding environment do not substantially alter aptamer-target recognition and binding, we employed the assay to detect and capture cancer cells with varying EpCAM expression levels. Because steric hindrance (i.e., protein density and/or clustering on the cell membrane) appears not to affect recognition, we hypothesized that the aptamer-EpCAM binding affinity is not altered among cells with low or high expression levels hence enabling us to quantify the expression levels of this biomarker in individual cells regardless of their EpCAM expression levels. Capturing cells on substrates and quantifying the biomarker expression has potential implications for use in enrichment of circulating tumor cells, exosome analysis, and personalized cancer treatment. Furthermore, it promises to be effective in the identification of outliers in populations of cells whose phenotype alterations might not be detectable with population-level techniques such as flow cytometry but might be important sentinels for early disease detection. While targeting cancer cells with aptamers uniquely selected to recognize membrane-expressed biomarkers is not an approach unique to us,[20,21] and although one previous report has shown that SERS can detect prostate cancer cells with high sensitivity using aptamers, our platform can quantify biomarker density in individual cells after effective capture and enrichment on the substrate enabled by truncated aptamers. In particular, by targeting EpCAM and monitoring slight variations in its expression, our approach could be implemented to follow quantitatively the evolution of cancerous tissues in real time. In particular, it could be important to follow their phenotype as they progress into metastatic lesions via epithelial-to-mesenchymal transition (EMT), in which EpCAM is down-regulated and markers of mesenchymal nature are overexpressed.

MATERIALS AND METHODS

Nanoparticle Synthesis. Gold nanostars were synthesized according to a modified version of the surfactant-free nanostar synthesis described by Yuan et al.[22] Briefly, 2 mL of $HAuCl_4$ salt solution (0.025 M) and 200 μL of 1 N HCl were added to 48 mL of Milli-Q water. A total of 125 μL of 12 nm citrate-capped spheres (A = 2.81) was then added to the mixture and mixed thoroughly by stirring. Then, 1 mL of 100 mM ascorbic acid and 2 mL of 3 mM $AgNO_3$ were simultaneously added to the above mixture. The reaction was carried out for 7 min under gentle stirring and then purified by centrifugation at 4000g for 10 min.

Table 1. Zeta Potential Values (mV) of Gold Nanostars Observed after Functionalization with 4-ATP and EpCAM Aptamer[a]

NP	zeta potential (mV)
NS in water	−37.3 ± 0.4
NS-4-ATP in water	51.8 ± 0.1
NS-4-ATP in PBS	9.7 ± 0.3
NS-4-ATP-Aptamer	−15.3 ± 0.1

[a]Results are shown as mean ± standard deviation with n = 3 readings for each sample.

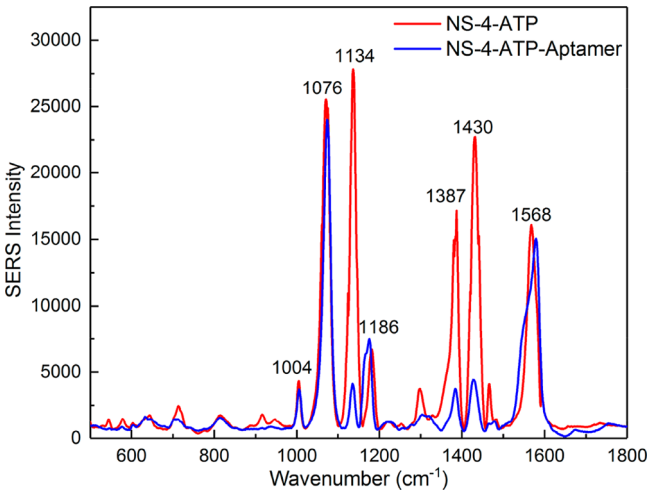

Figure 2. SERS spectra of 4-ATP coated nanostars and 4-ATP and EpCAM aptamer coated nanostars. Despite the introduction of additional peaks after functionalization with the thiolated aptamer, the peak at 1076 cm^{-1} is still dominant.

Table 2. SERS Peak Assignments for 4-Aminothiophenol between 500 and 2000 cm^{-1}[a]

SERS peaks	peak assignment
1614	δNH
1568	νCC
1495	νCC+δCH
1430	νCC+δCH
1387	δCH+ νCC
1298	νCC+δCH
1182	δCH
1134	δCH
1076	νCS
1004	γCC+γCCC
914	πCH
713	πCH+πCS+πCC

[a]The symbols δ, ν, and π correspond to bending, stretching, and wagging modes, respectively.

Preparation of SERS Tags. The thiolated EpCAM aptamer SYL3C (48-bp) developed by Song et al.[18] [5′-HS-$(CH_2)_6$- CAC TAC AGA GGT TGC GTC TGT CCC ACG TTG TCA TGG GGG GTT GGC CTG-Rhodamine Red-3′, Integrated DNA Technologies Inc.] was dissolved at 1 μM concentration in binding buffer (1X PBS, pH 7.4 with 4.5 g/L glucose and 5 mM $MgCl_2$) and treated with 50 mM Tris(2-carboxyethyl) phosphine hydrochloride (TCEP; Sigma-Aldrich) solution for 30 min at room temperature to eliminate disulfide bonds. A truncated SYL3C aptamer sequence (17-

DOI: 10.1021/acs.bioconjchem.8b00397
Bioconjugate Chem. XXXX, XXX, XXX−XXX

Scheme 1. Schematic Representation of the Sequence of Steps Followed To Carry out the Assay[a]

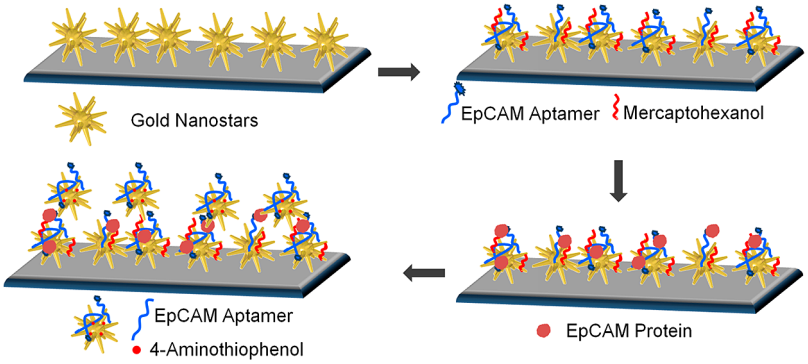

[a]Glass substrates, gold nanostars, EpCAM aptamer, mercaptohexanol, EpCAM protein, and 4-aminothiophenol are not drawn to scale.

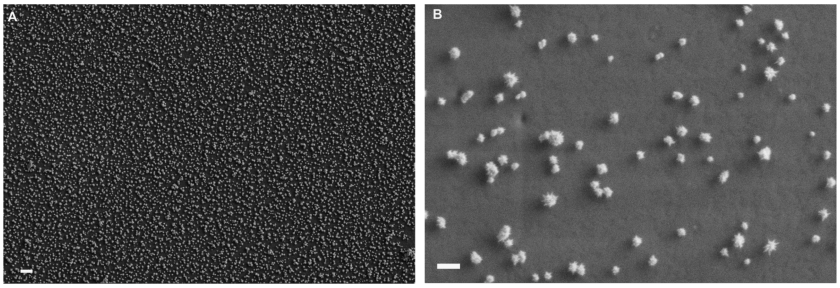

Figure 3. Scanning electron micrographs (SEM) of the substrate show uniform distribution of gold nanostars on its surface (A), with retained nanoparticle morphology (B). Slight reshaping is often induced by the electron beam. Scale bars are 1 μm in (A) and 200 nm in (B).

bp), EpA [5′-HS-$(CH_2)_6$-ACA GAG GTT GCG TCT GT-6-FAM-3′, Integrated DNA Technologies Inc.], developed by Macdonald et al.,[19] was also tested. For the preparation of SERS tags, the gold nanostars synthesized above were allowed to react for an additional 30 min with 1 mL of 50 mM solution of 4-aminothiophenol (Sigma-Aldrich). The nanoparticles were washed twice in water and resuspended at a final concentration of 3 nM in 1X PBS. 500 μL of the 3 nM nanostars was then allowed to react with 100 μL of 2 mg/mL sulfo-SMCC (Thermo Fisher) for 30 min. The nanoparticles were washed thoroughly and resuspended in 500 μL of 1X PBS. To this, 1 μM final concentration of EpCAM aptamer was added and allowed to react for 30 min. The SERS tags were washed twice and resuspended in the binding buffer.

Substrate Preparation. Glass microscope slides (Fisher Scientific; Plain microscope slides) were cut into approximately 0.5 cm × 1 cm sized substrates. They were rinsed thoroughly and sonicated for a few minutes in acetone and Milli-Q water. Following this step, they were immersed in a 2% solution of 3-aminopropyltriethoxysilane (APTES) for 20 min at room temperature. Afterward, they were placed in an oven set to 110 °C for 1 h. The substrates were then immersed in a 0.3% solution of bovine serum albumin (BSA) for 1 h following which they were washed thoroughly with Milli-Q water and left to dry overnight.

Surface Functionalization. The APTES functionalized substrates were incubated with a 3 nM gold nanostar solution for 1 h under gentle stirring. They were washed three times with Milli-Q water. Subsequently, the thiolated EpCAM aptamer at 1 μM concentration was deposited on the substrates and allowed to bind overnight. The substrates were then washed three times with Milli-Q water and incubated in a 1 mM 50% ethanolic solution of 6-mercaptohexanol (MCH) for 1 h. They were then washed three times with water and incubated with 40 μL of the desired concentration (10 pM to 3 μM concentration, prepared in binding buffer) of EpCAM protein (Thermo Fisher) for 1 h. They were then washed thoroughly and allowed to react with SERS tags for 1 h. The substrates were washed thoroughly to remove any unbound tags and allowed to dry before analyzing their SERS activity. The same procedure was repeated with BSA and fibrinogen as control proteins.

Characterization of NPs and SERS Tags. The functionalized nanoparticles were sonicated and redispersed prior to taking the measurements. The UV−vis spectra were recorded on an SI Photonics Model 440 spectrophotometer. The morphology of nanostars and SERS tags was evaluated using a Philips CM12 transmission electron microscope, and the size information was extracted using the ImageJ software. DLS and zeta potential measurements were performed using a Malvern Zetasizer Nano-ZS instrument. Three sequential measurements were performed for the experiments using water and 1X PBS diluent parameters with flow cell configuration. The zeta potential data were fit using Smoluchowski's theory.

Substrate Characterization. Noncontact mode AFM measurements were carried out with a Park systems NX10 AFM using a noncontact cantilever (PPP-NCHR, Park Systems) that had a force constant of 42 N/m (specific range: 10−130) and a resonant frequency of 330 kHz (specific range: 204−497). Scanning electron microscopy (SEM) images were collected using a Zeiss Sigma Field Emission SEM (Model 8100). All SERS measurements were carried out using a Renishaw in Via Raman microscope. The spectra were obtained with a 785 nm diode laser at a laser power of 0.17 mW using a data acquisition time of 10 s, single accumulation under a 50× objective. For each of the substrates, three maps

DOI: 10.1021/acs.bioconjchem.8b00397
Bioconjugate Chem. XXXX, XXX, XXX−XXX

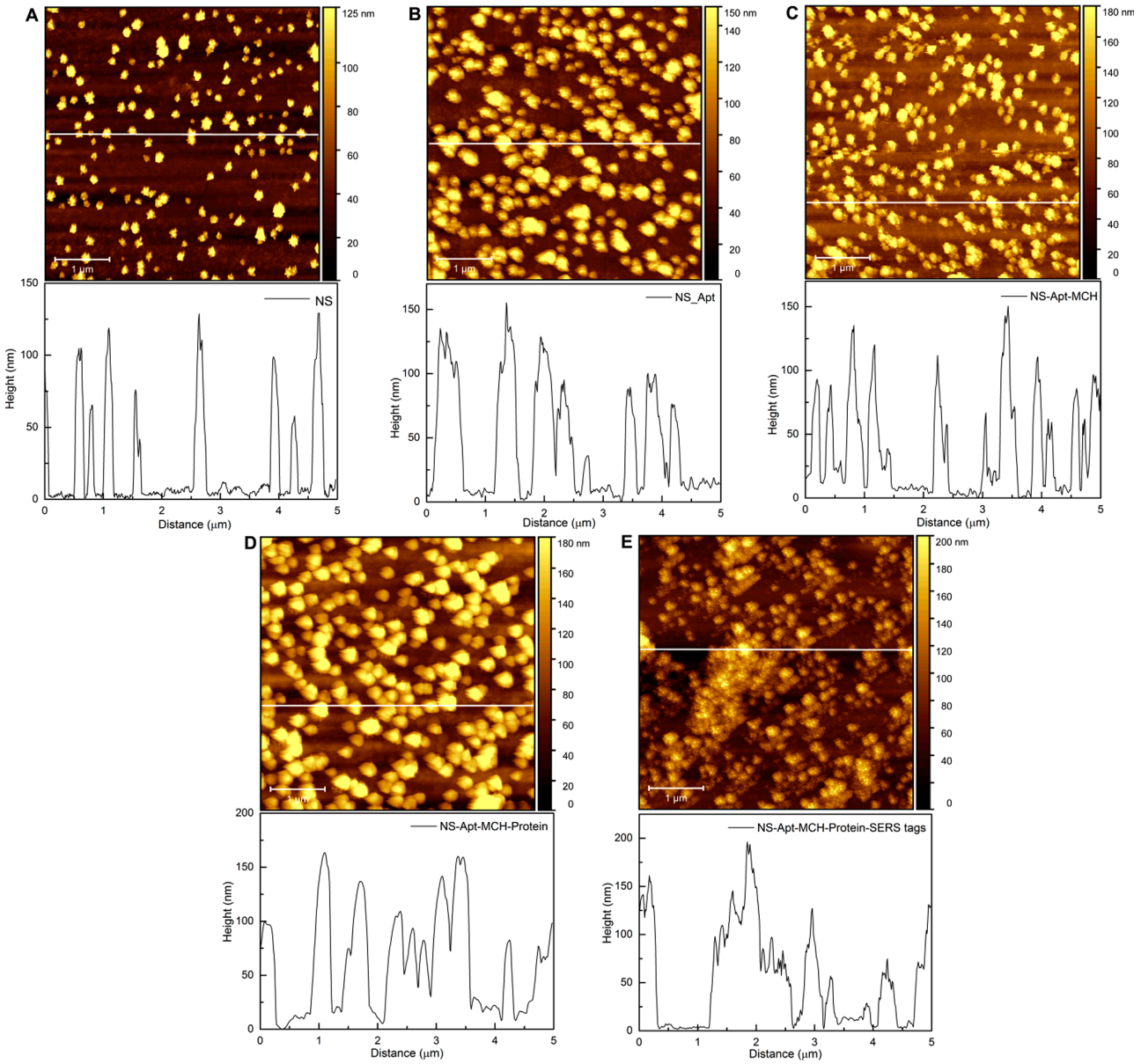

Figure 4. Topography and height profiles of the substrate at various functionalization steps collected via atomic force microscopy (AFM). (a) Substrate with nanostars only (h = 126 nm), (b) substrate with nanostars functionalized with EpCAM aptamer (h = 134 nm), (c) substrate with EpCAM-functionalized nanostars after addition of 6-mercaptohexanol (MCH) (h = 168 nm), (d) substrate with EpCAM- and MCH-functionalized nanostars after addition of EpCAM protein (h = 182 nm), and (e) after addition of SERS tags (h = 208 nm). A clear increase in the height profile can be observed at each stage. Height increase between steps C and D is a consequence of aptamer folding from its extended conformation in the self-assembled monolayer after recognition of the target protein.

of 5 × 5 μm^2 sized areas were chosen at random places of the sample. The areas were raster-scanned with a 1 μm step size. The final SERS spectra shown are averages of the three maps obtained. The intensity of a Si peak at 521 cm^{-1} was used as an internal reference. The limit of detection (LOD) for the protein and cell assays was calculated by ensuring that the SERS intensity peaks at the lowest concentration were three times higher than the intensities observed with the negative control samples.

Cell Culture. In this work, prostate cancer cells, PC-3, and breast cancer cells, MCF-7, were used as the target cell lines. Cervical cancer cells, HeLa, were used as an EpCAM-negative cell line. PC-3 cells were cultured in RPMI 1640 Media (Sigma-Aldrich) that was supplemented with 10% Fetal Bovine Serum (Gibco, Thermo Fisher Scientific), while MCF-7 cells and HeLa cells were cultured in Dulbecco's modified Eagle medium (Sigma) that was supplemented with 10% (v/v) Fetal Bovine Serum and 1% (v/v) penicillin-streptomycin (Thermo Fisher). Cells were grown at 37 °C with 5% CO_2. After reaching 70−80% confluency, the cells were trypsinized and resuspended in fresh media. For substrate capture experiments, the appropriate number of cells were counted and resuspended in 50 μL of 1X PBS and loaded onto the cell-capture substrates. After incubation at 37 °C for 1 h, the substrates were washed gently with 1X PBS. The captured cells were then allowed to react with SERS tags for another 1 h at 37 °C. The substrates were then washed thoroughly to remove unbound tags and fixed with 4% paraformaldehyde in PBS for 10 min. The captured cells on the substrate were then counted manually and detected by SERS measurements.

DOI: 10.1021/acs.bioconjchem.8b00397
Bioconjugate Chem. XXXX, XXX, XXX−XXX

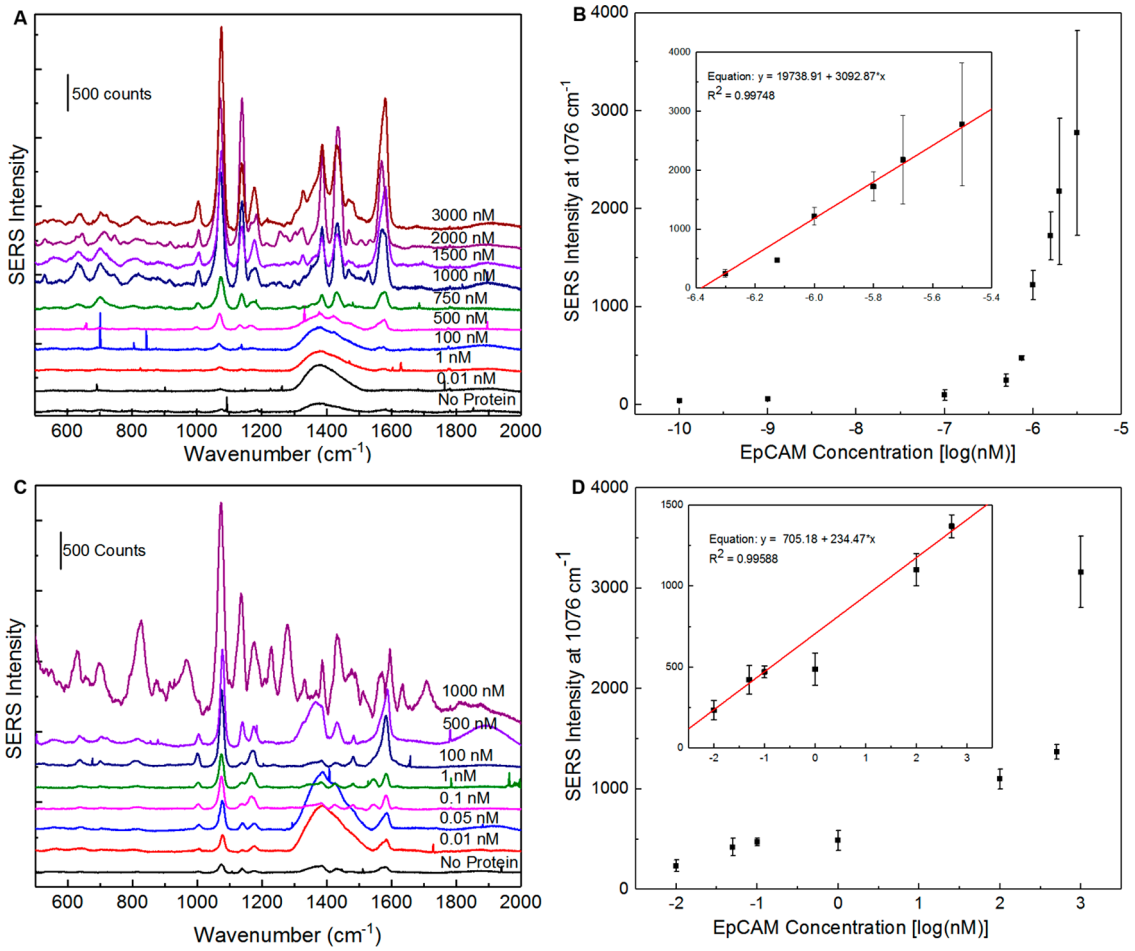

Figure 5. SERS spectra collected on the substrates after exposure to increasing concentrations of EpCAM. (A) and (C) show the SERS spectra for protein capture carried out with the 48-bp and the 17-bp EpCAM aptamers, respectively. (B) and (D) show the intensity variation of the 1076 cm^{-1} peak with respect to the EpCAM protein concentration (log (nM)), for the 48-bp and 17-bp aptamers, respectively. Inset figures show the linear dynamic range regime.

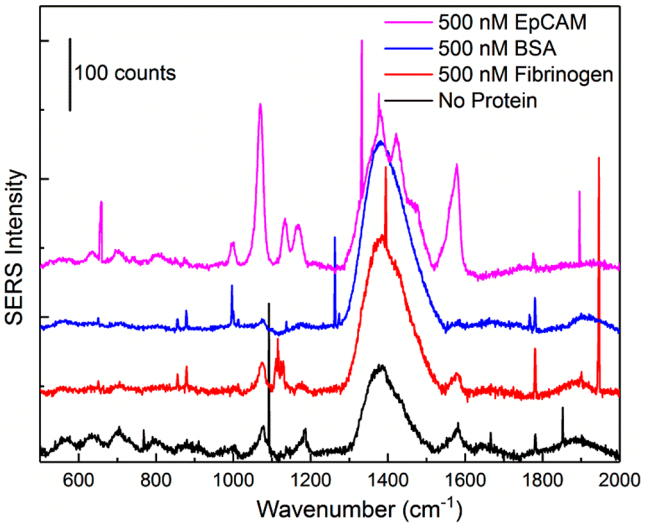

Figure 6. Assessment of assay selectivity. SERS spectra collected in the presence of 500 nM EpCAM and two control proteins, BSA and fibrinogen, in addition to the control without protein. The peak at ca. 1400 cm^{-1} is due to the interference of the glass substrate.

Flow Cytometry. After reaching 70−80% confluency, the three cell lines were dissociated with trypsin, washed, and resuspended in 1X PBS. They were then stained with anti-human EpCAM/TROP-1 PE conjugated antibody (R&D Systems) for 30 min at room temperature in the dark. Controls for the experiment contained unstained cells and isotype control cells that were stained with mouse IgG2B PE-conjugated antibody (R&D Systems). FACS analysis on the samples was carried out using a Beckman Coulter Gallios Flow Cytometry instrument, and the results were analyzed using Kaluza software.

NP and SERS Tags Synthesis. Gold nanostars were synthesized according to a modified version of the reported surfactant-free nanostar synthesis method[22] and were characterized by a localized surface plasmon resonance (LSPR) band centered at 745 nm. The morphology and size of all the particles were verified using TEM, as seen in Figure 1. TEM micrographs (Figure 1A and 1B) showed that the nanostars possessed a spherical core with a large number of sharp protruding spikes. The average tip-to-tip distance was measured to be 100.4 ± 24.4 nm.

The nanostars were then functionalized with 4-amino-thiophenol (4-ATP) and the thiolated EpCAM aptamer via coupling reactions mediated by sulfo-SMCC (succinimidyl 4-[*N*-maleimidomethyl]cyclohexane-1-carboxylate). Sulfo-SMCC is a heterobifunctional cross-linker that contains *N*-hydroxysuccinimide (NHS-ester) and maleimide groups that

DOI: 10.1021/acs.bioconjchem.8b00397
Bioconjugate Chem. XXXX, XXX, XXX−XXX

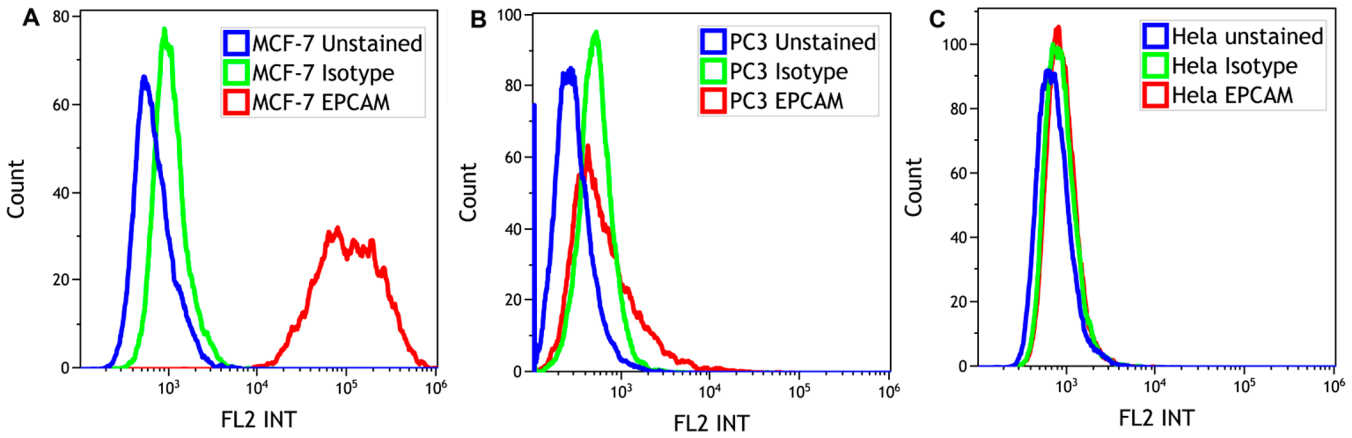

Figure 7. Flow cytometry results showing that MCF-7 and PC-3 cells are EpCAM positive cells, while HeLa are EpCAM negative cells.

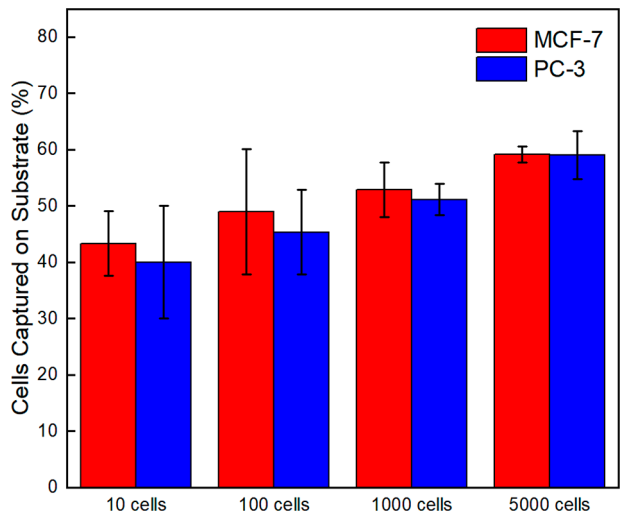

Figure 8. Cell capture efficiency (%) of the cancer cells, MCF-7 and PC-3, on the SERS substrates.

allow covalent conjugation to amine and sulfhydryl-containing molecules. The NHS-ester reacts with the primary amine of 4-ATP to form an amide bond, while the maleimide reacts with the thiol group on the EpCAM aptamer to form a stable thioether bond. TEM micrographs of the functionalized nanostars show that the sharp morphology of the particle is retained, thus ensuring that they will still be viable as SERS enhancing platforms (Figure 1B).

After surface functionalization, the nanostars showed an increase in size and a slight red shift in the LSPR position (Figure 1C). Because the position of the LSPR is dependent on the dielectric function of the attached ligand,[23] a shift indicates successful surface functionalization. In UV−vis spectroscopy experiments, the surfactant-free nanostars showed an LSPR around 745 nm that red-shifted to 773 nm upon addition of 4-ATP. Addition of the thiolated EpCAM aptamer caused a further red-shift to 787 nm. Furthermore, TEM micrographs shown in Figure 1B revealed an increase in the average size of the nanostars from 100.4 ± 24.4 nm (surfactant free stars) to 123.1 ± 16.3 nm for 4-ATP-EpCAM aptamer coated stars. This increase of 22.7 nm is consistent with the expected size contribution of the added 4-ATP reporter, SMCC, and the 48 bp EpCAM aptamer with its hairpin structure. In addition, dynamic light scattering (DLS) results (Figure 1D) also showed an increase in the hydrodynamic diameter of nanostars from 106.3 ± 0.4 nm to 119.1 ± 0.6 nm for 4-ATP coated nanostars and 140.6 ± 2.1 nm for nanostars functionalized with both 4-ATP and EpCAM aptamer. Aggregation of particles was observed after the synthesis of the SERS tags, as shown in Figure S3. The SERS tags were sonicated before each measurement to minimize aggregation.

The surface ligand exchange was further confirmed by a shift of ζ potential of the colloidal nanoparticles measured by the Zetasizer. The ζ potential is a measure of the electrophoretic mobility or net charge of nanoparticles. The results of the surface charges of the nanostars have been summarized in Table 1. We observed a shift in ζ potential from −37.3 ± 0.4 mV to 51.8 ± 0.1 mV after addition of 4-ATP to surfactant-free stars. The nanostars were then resuspended in 1X PBS at pH 7.4, at which point they displayed a surface charge of 9.7 ± 0.3 mV that then decreased to −15.3 ± 0.1 mV upon successful binding to the negatively charged thiolated EpCAM aptamer. The results seen were consistent with the expected charge contributions of 4-ATP and negatively charged DNA aptamer.

The addition of aptamer to the SERS tags was also confirmed using SERS. A solution of nanostars with 4-ATP and nanostars with 4-ATP and SYL3C aptamer was drop-casted onto a glass slide. The SERS measurements from each of the samples (average of three 5 μm × 5 μm maps) are shown in Figure 2. The SERS spectra of 4-ATP on nanostars showed strong peaks at 1076, 1182, 1387, 1430, and 1568 cm^{-1}. These peaks were assigned to νCS, δCH, δCH+νCC, νCC+δCH, and νCC respectively.[24−26] Upon addition of the aptamer to the 4-ATP functionalized nanostars, the peaks at 1136, 1382, and 1426 cm^{-1} shifted by less than 5 cm^{-1} and reduced in intensity indicating successful binding of the aptamer. The intense peak at 1076 cm^{-1}, corresponding to the stretching band of C−S bonds in 4-ATP molecules, was still prominent after aptamer addition and was therefore chosen for concentration studies with soluble EpCAM protein. All the SERS peak assignments for 4-ATP have been summarized in Table 2.

Substrate Preparation. The overall procedure for the design of the substrate to capture EpCAM protein is shown in Scheme 1. The first step after silanization of the glass slides is the addition of gold nanostars. We chose a concentration of 3 nM which ensured a uniform nanostar distribution without substantial clustering. The distribution of unmodified nanostars on the surface of the substrate was visualized by scanning

DOI: 10.1021/acs.bioconjchem.8b00397
Bioconjugate Chem. XXXX, XXX, XXX−XXX

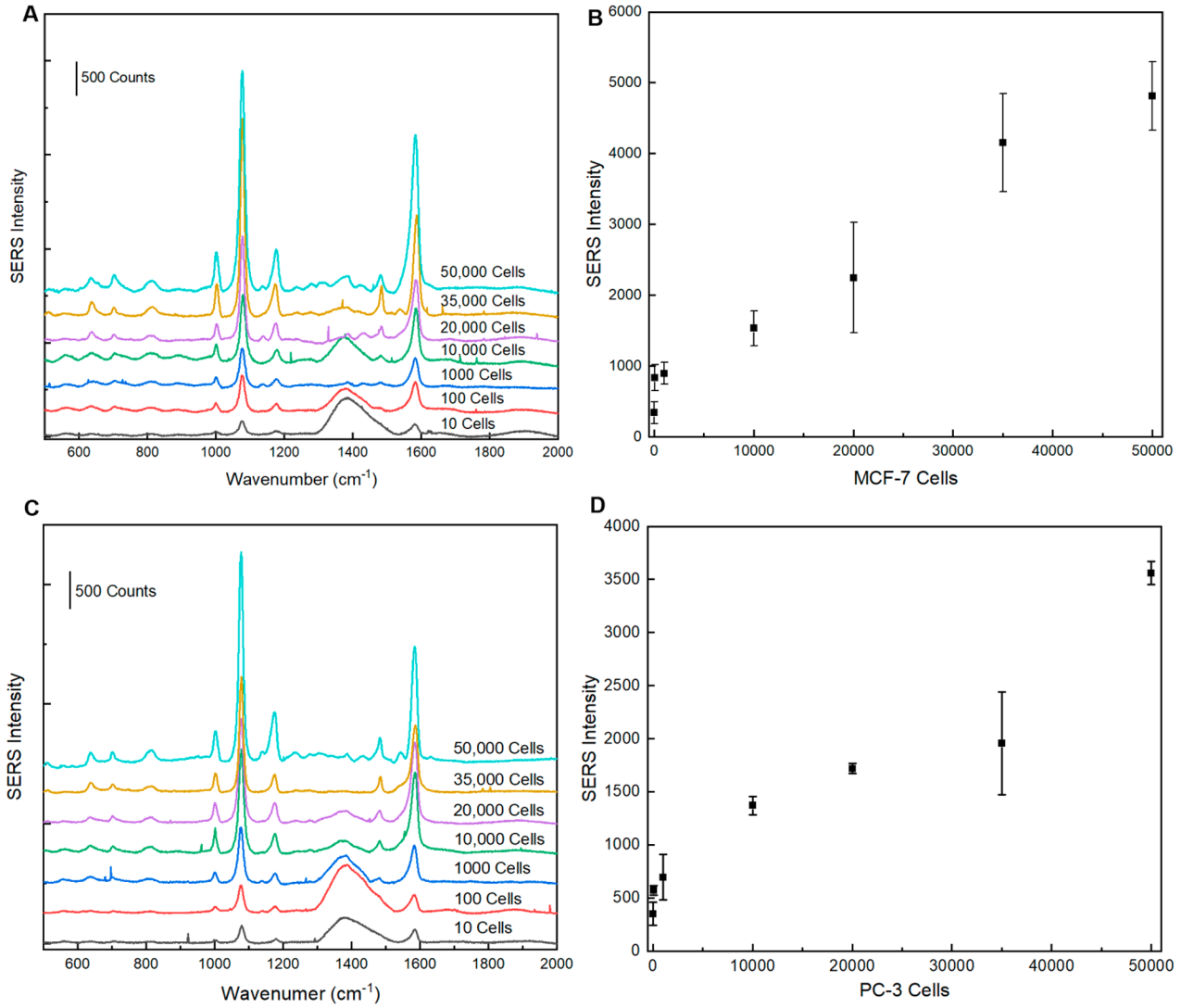

Figure 9. Quantification of MCF-7 (A, B) and PC-3 (C, D) cells using the described assay. By monitoring the intensity of the 1076 cm^{-1} peak (A), it can be observed how the SERS response increases with the number of MCF-7 cells between the wavenumbers 500 and 2000 cm^{-1} (B). A similar dependence is observed between the intensity of the 1076 cm^{-1} peak and the number of PC-3 cells (C and D). The data were fit using a 3-parameter logistic binding, as detailed in Figure S6.

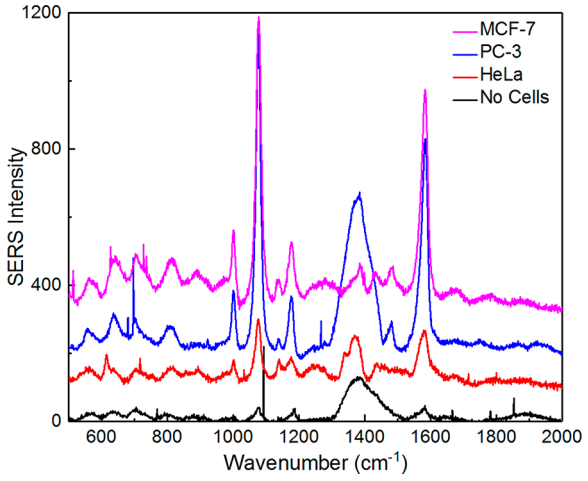

Figure 10. Assessment of assay selectivity on cells with different membrane expression of EpCAM (MCF-7 and PC3) or with no expressed EpCAM. A control spectrum without cells is also shown.

electron microscopy (SEM), as seen in Figure 3. The second step in the substrate preparation was the *in situ* functionalization with the suitable aptamer. We chose a 48 bp SYL3C sequence against EpCAM, which is a trihairpin structured sequence with strong binding affinity and selectivity against cancer cells expressing EpCAM (Figure S1).[18] The aptamer sequence was designed to possess a thiol group to enable binding to the surface of the gold nanostars. In order to optimize aptamer-protein recognition while avoiding nonspecific binding, the substrate was backfilled with 6-mercaptohexanol (MCH). The presence of MCH prevents nonspecific adsorption of the aptamer to the gold surface and improves the binding efficiency of the aptamer to its target.[27] The substrates were later incubated with varying concentrations of EpCAM protein that was prepared in the binding buffer specific for this aptamer-target pair (1X PBS, pH 7.4 with 4.5 g/L glucose and 5 mM $MgCl_2$) and allowed to interact. The final step in the substrate preparation was the addition of SERS tags to identify and localize aptamer-protein binding events.

DOI: 10.1021/acs.bioconjchem.8b00397
Bioconjugate Chem. XXXX, XXX, XXX−XXX

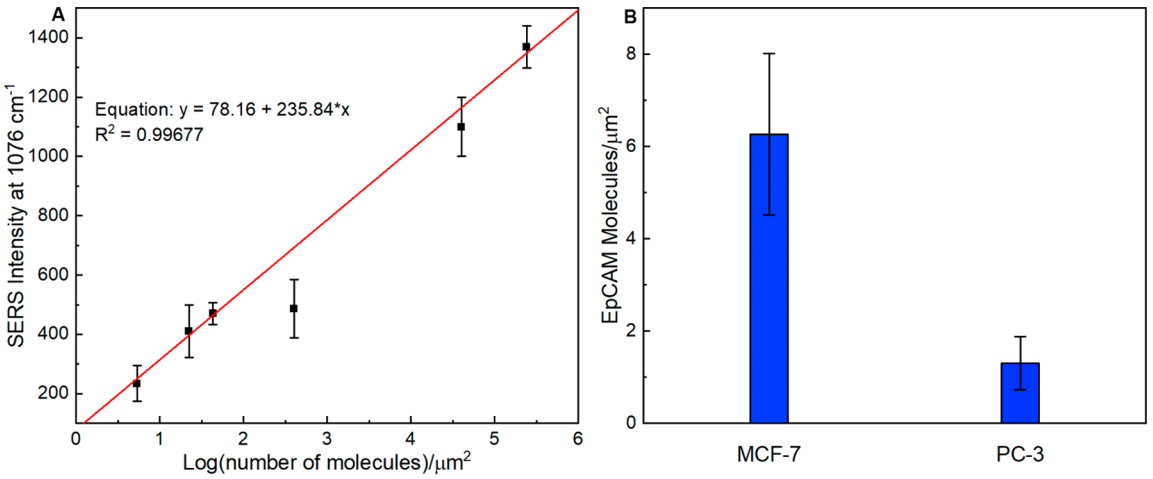

Figure 11. Quantification of EpCAM density in individual cells. (A) shows the linear correlation (R^2 = 0.99677) between log of the number of EpCAM molecules found per μm^2 area at different protein concentrations and their SERS response at 1076 cm^{-1}. Using this equation, the number of EpCAM molecules present per μm^2 area on MCF-7 and PC-3 cells was calculated and shown in (B). Higher expression levels are observed in MCF-7 cells, as expected.

AFM Measurements. Atomic force microscopy (AFM) measurements (5 × 5 μm^2 area) were carried out on the substrates to analyze surface features emerging and/or disappearing at each step of the substrate preparation. The images in Figure 4 provide an overview of distribution and binding of each reagent on the developed substrates and show the height profile at each functionalization step. Figure 4A shows the first step after addition of gold nanostars to a glass slide. At this stage, the substrates show an average height of 126 nm which is consistent with the size of nanostars measured via TEM. Thiolated EpCAM aptamers at 1 μM concentration were then deposited onto the substrate (Figure 4B), which showed an average height increase of 8 nm. This height could correspond to the presence of several aptamer strands lying flat on the surface of nanostars, possibly due to G-rich, ribbon-like structures that might have formed as a result of the high GC content (60.4%) in the aptamer sequence, as well as of nonspecific adsorption of the nucleotide bases to the gold surface.[27,28] Therefore, we determined that a spacer such as MCH was necessary to remove nonspecific binding and evenly distribute the aptamer across the substrate to improve target binding and identification. Upon addition of MCH, a redistribution of the aptamer strands was observed, as seen in Figure 4C. As expected, the addition of MCH eliminates nonspecific adsorption of the aptamer on the gold nanoparticle surface[27] resulting in a height change of 34 nm, which corresponds to the length of the aptamer (inclusive of the C6 spacer and the rhodamine red dye) in its extended form. The substrates were then treated with 500 nM EpCAM protein (Figure 4D), which caused an increase in height to 182 nm. The observed 14 nm increase in height is likely due to the capture of two protein molecules on the surface of nanostars. Finally, SERS tags were added to the substrate (Figure 4E). The areas where the SERS tags recognized and bonded the protein showed a height of 208 nm, while the rest of the substrates did not see a change in height. In the last two steps, we observed that the binding of the protein to the aptamer on the substrates was uneven, implying that the recognition of the target by the aptamer sequence could be different when occurring on a substrate, as opposed to when both the aptamer and the target are in suspension.

SERS Measurements. SERS measurements of different concentrations of EpCAM protein recognized and captured by the SYL3C aptamer were carried out on the prepared substrates. From Figure 5, it is evident that the SERS intensity increased as the concentration of the soluble EpCAM protein increased, as, in turn, more SERS tags were captured by increasing amounts of protein recognized in the sandwich assay. Control experiments ensured that the spectra obtained from the substrates originated from the Raman reporter, 4-ATP, only and that the EpCAM aptamer and the protein did not contribute to any SERS peaks (Figure S4). Figure 5B shows the intensity of the characteristic Raman band of 4-ATP at 1076 cm^{-1} varying with the concentration of EpCAM protein added to the substrates. Each data point represents the average of three 5 μm × 5 μm maps collected randomly on each substrate. Further analysis showed a linear correlation (R^2 = 0.996) between SERS intensity and the log of the EpCAM protein concentration in nM between the concentrations of 500 nM and 3 μM with a calibration curve characterized by the equation $y = 19738.91 + 3092.87x$.

In order to test the selectivity of the EpCAM aptamer, we chose two control proteins, bovine serum albumin (BSA) and fibrinogen, at a concentration of 500 nM each. The SERS intensity obtained from the substrates of each of the control proteins was then compared to the intensity of EpCAM protein at 500 nM (Figure 6). Both control proteins showed a much lower intensity at the characteristic peak of 1076 cm^{-1} when compared to the EpCAM protein at the same concentration. These results indicate that the substrates developed with the SYL3C EpCAM aptamer have specificity only for EpCAM protein. The limit of detection for the assay was found to be at a concentration where the SERS intensity values at 1076 cm^{-1} were at least three times higher than the no-protein control group. For our protein assay using the SYL3C EpCAM aptamer, the detection limit was found to be between 100 nM and 500 nM. We wondered if the structure of the hairpin loops formed by the aptamer at the incubation temperature (room temperature) played a role in its sensitivity. Using the OligoAnalyzer 3.1 tool (Integrated DNA Technologies, Inc.), we found that 7 different configurations (Figure S1) of the three hairpin loops are similarly favored energeti-

DOI: 10.1021/acs.bioconjchem.8b00397
Bioconjugate Chem. XXXX, XXX, XXX−XXX

cally at 25 °C, making it likely for them to be rapidly interconverting. Since the recognition of the protein by the aptamer depends on both conformational and electrostatic interactions between oligonucleotide and target, it is likely that the conformational conversions might impact effective target recognition and binding, thus affecting assay sensitivity. In order to reduce the possible configurations at the incubation temperature, and thus improve the sensitivity of the assay, we used a truncated aptamer sequence that was developed from the SYL3C sequence. The shorter 17 bp EpA aptamer has a single hairpin loop with only 2 possible secondary configurations at 25 °C, which reduces the possibility of conformational changes at room temperature hence increasing sensitivity. The shorter aptamer was found to lead to higher assay sensitivity when compared to the longer SYL3C EpCAM aptamer.[19] We tested the binding affinity of the shorter EpA aptamer sequence using different concentrations of EpCAM protein (500 nM to 10 pM) and determined two dissociation constants (k_{D1} = 0.02 nM and k_{D2} = 48.78 nM) for the 10 pM−1 nM and 1 nM−500 nM concentration regimes, respectively, using a 3-parameter logistic binding model (see Figure S5), recommended to fit data from ELISA assays.[29] We found that at the two highest concentrations, the SERS intensities obtained with the shorter EpA aptamer (Figure 5C) were found to be 3-fold higher at 1 μM and 5.7 times higher at 500 nM protein concentration when compared to the SYL3C aptamer in the same conditions. In addition to higher intensities, the shorter EpA aptamer sequence exposed to 1 μM EpCAM protein showed additional peaks at 1229, 1276, 1633, and 1707 cm^{-1}, which we assigned to the SERS peaks of 6-FAM that is present at the 3′ *terminus* of the 17 bp aptamer sequence (Figure S2). At this protein concentration, it could be possible for the dye to interact differently with the active metallic surface compared to what was observed at lower concentrations of protein. Since SERS is a tensorial technique, the conformation of the reporter molecule and its presentation with respect to the metallic surface are important. Thus, the additional peaks suggest that aptamer folding might depend not only on the concentration and packing of the aptamer on the metallic surface but also on its interaction with the target protein. Like the SYL3C aptamer, the shorter aptamer sequence also showed a linear correlation (R^2 = 0.995) between SERS intensity and the log of the EpCAM protein concentration in nM (Figure 5D) between the concentrations of 10 pM and 500 nM with a calibration curve that is represented by the equation $y = 705.108 + 234.47x$. The lowest concentration of protein that we could detect with the EpA-conjugated substrates was 10 pM. This detection limit was chosen because the SERS intensity of the 1076 cm^{-1} peak was three times higher than the no-protein control. Because of the improved sensitivity it enabled, the EpA aptamer was chosen for further experiments in cancer cells.

For the cell capture experiments, we chose two EpCAM positive cell lines, a breast cancer cell line, MCF-7 and a prostate cancer cell line, PC-3. These cells were chosen because of the different levels of EpCAM biomarker expressed on their cell surfaces. In addition to these two EpCAM positive cell lines, an EpCAM negative cell line, HeLa, was chosen as a negative control. The surface expression of EpCAM on all three cells was confirmed via flow cytometry. The results from these experiments (Figure 7) confirmed that MCF-7 cells have higher expression of EpCAM when compared to PC-3 cells and that HeLa cells do not express the biomarker. However, population-averaged results cannot provide the single-cell insight that is necessary to pinpoint the presence of abnormal cells, for instance cells that are undergoing epithelial to mesenchymal transition, which are often encountered in very low numbers. Thus, leveraging the promising results obtained with the described nanostar-based assay, we ran a set of experiments aimed at quantifying, at the single cell level, the expression of specific cancer cell biomarkers.

Upon confirmation of expression of EpCAM on cell surfaces, the desired numbers of MCF-7 and PC-3 cells (10 cells to 50,000 cells) were counted and resuspended in 50 μL of 1X PBS and loaded onto the substrates. After incubation at 37 °C for 1 h, the substrates were washed and fixed. The capture yields of cells between 10 and 5000 cells were then evaluated by counting the captured cells under a bright field microscope (Figure 8). For both cell lines, at low cell counts (10 cells), a capture efficiency of around 40% was observed. Upon increasing cell numbers, the capture efficiency increased, as expected.[30,31] Overall, slightly more MCF-7 cells were captured when compared to PC-3 cells. This could be attributed to the higher EpCAM expression seen on MCF-7 cells. Above a cell count of 5000 cells, the capture efficiency for both cell lines was found to be greater than 60%. On the other hand, a very low capture (0.067%) was seen with the EpCAM negative cell line, HeLa, when 1000 cells were added to the substrate.

The captured cells were then labeled with SERS tags for SERS measurements. Both MCF-7 cells and PC-3 cells showed an enhancement of the characteristic peak of 4-ATP at 1076 cm^{-1} (Figure 9) which increased linearly with increasing cell numbers between 100 cells and 50,000 cells. The detection limit with these substrates was found to be 10 cells, which was calculated the same way as the protein assays. The absolute SERS intensity values used for determining the limit of detection of the protein and cell assays have been shown in Table S1. Higher SERS intensities were observed with MCF-7 cells when compared to PC-3 cells, in agreement with flow cytometry results. In addition, the substrates showed very low SERS enhancement (Figure 10) at a concentration of 1000 cells with the EpCAM negative cells, HeLa, when compared to the two positive cell lines at the same concentration.

In order to estimate the number of EpCAM molecules present on the cancer cells, we calculated the number of EpCAM molecules at different concentrations based on the calibration curve reported in Figure 5(D). The number of molecules at each concentration was calculated using the following equation:

$$(\text{Concentration (M)} \times (6.023*10^{23}) \times \text{Volume of Protein Added (L)}) / \text{Surface Area of Substrate } (\mu m^2)$$

A linear correlation (R^2 = 0.99677) was then observed between the log of the number of protein molecules per μm^2 area of the cell and the SERS intensity as shown in Figure 11(A). The relation was represented by the equation $y = 78.16 + 235.84x$. Using this equation and the SERS intensity of MCF-7 and PC-3 cells observed at 1076 cm^{-1}, we calculated the number of EpCAM molecules expressed by the two cell types at the single cell level. The number density (per μm^2) of EpCAM molecules present on MCF-7 cells was found to be 4.8-fold higher than that of PC-3 cells (Figure 11(B)).

DOI: 10.1021/acs.bioconjchem.8b00397
Bioconjugate Chem. XXXX, XXX, XXX−XXX

CONCLUSION

In conclusion, we developed a SERS-based substrate for the recognition and quantification of EpCAM protein, both soluble and cell membrane-embedded. By leveraging the field-enhancing properties of gold nanostars and the improved recognition and capture enabled by truncated aptamers designed for cell-expressed EpCAM, we detected soluble EpCAM with limits of detection of 10 pM, thus further proving that aptamers designed using cell-SELEX approaches are effective also for the recognition of soluble proteins. By employing the same substrate, we demonstrated that identification and quantification of biomarker expression can be achieved at the single cell level, enabling one to discern among cells with varying phenotype expression levels. This capability allows one to foresee how our approach could be relevant for early cancer detection or for monitoring the onset of metastasis, for which the isolation of individual cells with altered phenotype from populations of cells with uniform biomarker expression is challenging, if not impossible, with techniques such as flow cytometry. Although we have here reported a study targeting EpCAM, it is easy to envision how any biomarker of interest could be targeted, both individually and in multiplex, by simply functionalizing the substrate and the SERS tags with the appropriate aptamers. Importantly, this diagnostic approach does not require protein labeling and, owing to the enhancement capabilities of the nanostar-based substrate, could be implemented with portable Raman spectrometers, making its implementation in the clinic or at bedside more likely to become a reality.

ASSOCIATED CONTENT

Supporting Information

The Supporting Information is available free of charge on the ACS Publications website at DOI: 10.1021/acs.bioconjchem.8b00397.

Different secondary configurations of the 48 bp and 17 bp EpCAM DNA aptamers at room temperature, SERS peaks of 6-FAM dye using 633 and 785 nm laser, dynamic light scattering (DLS) results of the SERS tags with and without sonication, SERS peaks arising from the EpCAM aptamer and the EpCAM protein, determination of limit of detection of the protein and cell assays (PDF)

AUTHOR INFORMATION

Corresponding Author

*E-mail: lfabris@soe.rutgers.edu.

ORCID

Hyeon-Yeol Cho: 0000-0003-1897-1166

Laura Fabris: 0000-0002-7089-5175

Notes

The authors declare no competing financial interest.

ACKNOWLEDGMENTS

This work was funded through Rutgers Busch Biomedical Grant 17030517. Acquisition of the atomic force microscope was funded by National Science Foundation Grant CHE-1429062. We thank Prof. Isaac Kim (Chief, Urologic Oncology, Rutgers Cancer Institute of New Jersey) and Dr. Geuntaek Lee (Instructor, Urologic Oncology, Rutgers Cancer Institute of New Jersey) for giving us access to their tissue culture facilities and their PC3 cell line. The insight they provided during the course of the project is greatly appreciated.

REFERENCES

(1) Ferrari, M. (2005) Cancer nanotechnology: opportunities and challenges. *Nat. Rev. Cancer 5*, 161−71.

(2) Sawyers, C. L. (2008) The cancer biomarker problem. *Nature 452*, 548−52.

(3) Went, P., Vasei, M., Bubendorf, L., Terracciano, L., Tornillo, L., Riede, U., Kononen, J., Simon, R., Sauter, G., and Baeuerle, P. A. (2006) Frequent high-level expression of the immunotherapeutic target Ep-CAM in colon, stomach, prostate and lung cancers. *Br. J. Cancer 94*, 128−35.

(4) Spizzo, G., Went, P., Dirnhofer, S., Obrist, P., Moch, H., Baeuerle, P. A., Mueller-Holzner, E., Marth, C., Gastl, G., and Zeimet, A. G. (2006) Overexpression of epithelial cell adhesion molecule (Ep-CAM) is an independent prognostic marker for reduced survival of patients with epithelial ovarian cancer. *Gynecol. Oncol. 103*, 483−8.

(5) Gorges, T. M., Tinhofer, I., Drosch, M., Röse, L., Zollner, T. M., Krahn, T., and von Ahsen, O. (2012) Circulating tumour cells escape from EpCAM-based detection due to epithelial-to-mesenchymal transition. *BMC Cancer 12*, 178.

(6) Bantz, K. C., Meyer, A. F., Wittenberg, N. J., Im, H., Kurtulus, O., Lee, S. H., Lindquist, N. C., Oh, S. H., and Haynes, C. L. (2011) Recent progress in SERS biosensing. *Phys. Chem. Chem. Phys. 13*, 11551−67.

(7) Wang, Y., Yan, B., and Chen, L. (2013) SERS Tags: Novel Optical Nanoprobes for Bioanalysis. *Chem. Rev. 113*, 1391−1428.

(8) Huang, R., Harmsen, S., Samii, J. M., Karabeber, H., Pitter, K. L., Holland, E. C., and Kircher, M. F. (2016) High Precision Imaging of Microscopic Spread of Glioblastoma with a Targeted Ultrasensitive SERRS Molecular Imaging Probe. *Theranostics 6*, 1075−84.

(9) Cho, H. Y., Hossain, M. K., Lee, J. H., Han, J., Lee, H. J., Kim, K. J., Kim, J. H., Lee, K. B., and Choi, J. W. (2018) Selective isolation and noninvasive analysis of circulating cancer stem cells through Raman imaging. *Biosens. Bioelectron. 102*, 372−382.

(10) Rodríguez-Lorenzo, L., Álvarez-Puebla, R. A., de Abajo, F. J. G., and Liz-Marzán, L. M. (2010) Surface Enhanced Raman Scattering Using Star-Shaped Gold Colloidal Nanoparticles. *J. Phys. Chem. C 114*, 7336−7340.

(11) Tuerk, C., and Gold, L. (1990) Systematic evolution of ligands by exponential enrichment: RNA ligands to bacteriophage T4 DNA polymerase. *Science 249*, 505−10.

(12) Ellington, A. D., and Szostak, J. W. (1992) Selection in vitro of single-stranded DNA molecules that fold into specific ligand-binding structures. *Nature 355*, 850−852.

(13) Lee, J. H., Yigit, M. V., Mazumdar, D., and Lu, Y. (2010) Molecular diagnostic and drug delivery agents based on aptamer-nanomaterial conjugates. *Adv. Drug Delivery Rev. 62*, 592−605.

(14) Pang, X., Cui, C., Wan, S., Jiang, Y., Zhang, L., Xia, L., Li, L., Li, X., and Tan, W. (2018) Bioapplications of Cell-SELEX-Generated Aptamers in Cancer Diagnostics, Therapeutics, Theranostics and Biomarker Discovery: A Comprehensive Review. *Cancers 10*, 47.

(15) Shangguan, D., Meng, L., Cao, Z. C., Xiao, Z., Fang, X., Li, Y., Cardona, D., Witek, R. P., Liu, C., and Tan, W. (2008) Identification of liver cancer-specific aptamers using whole live cells. *Anal. Chem. 80*, 721−8.

(16) Que-Gewirth, N. S., and Sullenger, B. A. (2007) Gene therapy progress and prospects: RNA aptamers. *Gene Ther. 14*, 283−91.

(17) Yoon, S., and Rossi, J. J. (2018) Targeted Molecular Imaging Using Aptamers in Cancer. *Pharmaceuticals 11*, 71.

(18) Song, Y., Zhu, Z., An, Y., Zhang, W., Zhang, H., Liu, D., Yu, C., Duan, W., and Yang, C. J. (2013) Selection of DNA Aptamers against Epithelial Cell Adhesion Molecule for Cancer Cell Imaging and Circulating Tumor Cell Capture. *Anal. Chem. 85*, 4141−4149.

(19) Macdonald, J., Henri, J., Goodman, L., Xiang, D., Duan, W., and Shigdar, S. (2017) Development of a Bifunctional Aptamer Targeting the Transferrin Receptor and Epithelial Cell Adhesion

DOI: 10.1021/acs.bioconjchem.8b00397
Bioconjugate Chem. XXXX, XXX, XXX−XXX

Molecule (EpCAM) for the Treatment of Brain Cancer Metastases. *ACS Chem. Neurosci. 8*, 777−784.
(20) Dam, D. H. M., Culver, K. S. B., and Odom, T. W. (2014) Grafting Aptamers onto Gold Nanostars Increases in Vitro Efficacy in a Wide Range of Cancer Cell Types. *Mol. Pharmaceutics 11*, 580−587.
(21) Lu, W., Singh, A. K., Khan, S. A., Senapati, D., Yu, H., and Ray, P. C. (2010) Gold Nano-Popcorn-Based Targeted Diagnosis, Nanotherapy Treatment, and In Situ Monitoring of Photothermal Therapy Response of Prostate Cancer Cells Using Surface-Enhanced Raman Spectroscopy. *J. Am. Chem. Soc. 132*, 18103−18114.
(22) Yuan, H., Khoury, C. G., Hwang, H., Wilson, C. M., Grant, G. A., and Vo-Dinh, T. (2012) Gold nanostars: surfactant-free synthesis, 3D modelling, and two-photon photoluminescence imaging. *Nanotechnology 23*, 075102.
(23) Maier, S. A. (2007) *Plasmonics: fundamentals and applications*, Springer Science & Business Media, DOI: 10.1007/0-387-37825-1.
(24) Hu, X., Wang, T., Wang, L., and Dong, S. (2007) Surface-Enhanced Raman Scattering of 4-Aminothiophenol Self-Assembled Monolayers in Sandwich Structure with Nanoparticle Shape Dependence: Off-Surface Plasmon Resonance Condition. *J. Phys. Chem. C 111*, 6962−6969.
(25) Quynh, L. M., Nam, N. H., Kong, K., Nhung, N. T., Notingher, I., Henini, M., and Luong, N. H. (2016) Surface-Enhanced Raman Spectroscopy Study of 4-ATPon Gold Nanoparticles for Basal Cell CarcinomaFingerprint Detection. *J. Electron. Mater. 45*, 2563−2568.
(26) Osawa, M., Matsuda, N., Yoshii, K., and Uchida, I. (1994) Charge transfer resonance Raman process in surface-enhanced Raman scattering from p-aminothiophenol adsorbed on silver: Herzberg-Teller contribution. *J. Phys. Chem. 98*, 12702−12707.
(27) Steel, A. B., Levicky, R. L., Herne, T. M., and Tarlov, M. J. (2000) Immobilization of nucleic acids at solid surfaces: effect of oligonucleotide length on layer assembly. *Biophys. J. 79*, 975−81.
(28) Davis, J. T., and Spada, G. P. (2007) Supramolecular architectures generated by self-assembly of guanosine derivatives. *Chem. Soc. Rev. 36*, 296−313.
(29) Nummer, S. A., Weeden, A. J., Shaw, C., Snyder, B. K., Bridgeman, T. B., and Qian, S. S. (2018) Updating the ELISA standard curve fitting process to reduce uncertainty in estimated microcystin concentrations. *MethodsX 5*, 304−311.
(30) Zhang, P., Zhang, R., Gao, M., and Zhang, X. (2014) Novel nitrocellulose membrane substrate for efficient analysis of circulating tumor cells coupled with surface-enhanced Raman scattering imaging. *ACS Appl. Mater. Interfaces 6*, 370−6.
(31) Wang, S., Wang, H., Jiao, J., Chen, K. J., Owens, G. E., Kamei, K., Sun, J., Sherman, D. J., Behrenbruch, C. P., Wu, H., et al. (2009) Three-dimensional nanostructured substrates toward efficient capture of circulating tumor cells. *Angew. Chem., Int. Ed. 48*, 8970−3.

DOI: 10.1021/acs.bioconjchem.8b00397
Bioconjugate Chem. XXXX, XXX, XXX−XXX